# Weakly anisotropic frustrated zigzag spin chain

D. V. Dmitriev* and V. Ya. Krivnov
*Joint Institute of Chemical Physics, RAS, Kosygin Strasse 4, 119334 Moscow, Russia*
(Received 28 August 2007; published 2 January 2008)

The frustrated spin-1/2 model with weakly anisotropic ferromagnetic nearest-neighbor and antiferromagnetic next-nearest-neighbor exchanges is studied with use of variational mean-field approach, scaling estimates of the infrared divergencies in the perturbation theory and finite-size calculations. The ground-state phase diagram of this model contains three phases: the ferromagnetic phase, the commensurate spin-fluid phase, and the incommensurate phase. The nontrivial behavior of the boundaries between these phases and the character of the phase transitions in case of weak anisotropy are determined.

DOI: 10.1103/PhysRevB.77.024401 PACS number(s): 75.10.Jm

## I. INTRODUCTION

The quantum spin chains with nearest-neighbor (NN) $J_1$ and next-nearest-neighbor (NNN) interactions $J_2$ have been a subject of numerous studies.[1] The model with both antiferromagnetic interactions $J_1,J_2>0$ (AF-AF model) is well studied.[2–7] Lately, there has been considerable interest in the study of F-AF model with the ferromagnetic NN and the antiferromagnetic NNN interactions ($J_1<0$, $J_2>0$).[8–14] One of the reasons is understanding of intriguing magnetic properties of a novel class of edge-sharing copper oxides which are described by the F-AF model.[15–20] In particular, these copper oxides show at low temperature a tendency to the formation of the incommensurate state with helicoidal magnetic ordering.

The Hamiltonian of the spin-1/2 F-AF model is

$$H=-\sum_{n=1}^{N}(S_n^xS_{n+1}^x+S_n^yS_{n+1}^y+\Delta_1S_n^zS_{n+1}^z)$$
$$+J\sum_{n=1}^{N}(S_n^xS_{n+2}^x+S_n^yS_{n+2}^y+\Delta_2S_n^zS_{n+2}^z), \qquad (1)$$

where we set $J_1=-1$ and $J_2=J>0$, and the periodic boundary conditions are implied.

The isotropic case of this model ($\Delta_1=\Delta_2=1$) is intensively studied in last years.[11,12,21–23] It is known that the ground state of the isotropic version of model (1) is ferromagnetic for $0<J<1/4$, and it becomes a singlet incommensurate state for $J>1/4$.[24,25] The phase transition at $J=1/4$ is the second-order one.

The model with the anisotropy of exchange interactions is less studied, especially for the case of the small anisotropy. For example, the phase diagram of model (1) with $\Delta_1=\Delta_2$ has been studied in Ref. 26 using the method of level spectroscopy. Unfortunately, this method becomes unreliable for $J\approx1/4$ and $\Delta_1=\Delta_2\approx1$ because of strong finite-size effects.

In real chain compounds, the exchange interactions are anisotropic. The microscopic origin of these interactions is the spin-orbit coupling. The indication on the anisotropy is a dependence of the saturation field on the direction of the external magnetic field.[16] Though, as a rule, the anisotropy is weak (for example, for edge-shared cuprate $LiCuVO_4$, electron spin resonance detected a 6% anisotropy[27]), it can change the transition point from commensurate to incommensurate states as well as the behavior of model (1) in the vicinity of the transition point. Besides, the frustration parameter $|J_2/J_1|=J$ estimated for some edge-sharing copper oxides is close to the quantum critical point 1/4 [for example, $J\sim0.28-0.3$ for compound $Li_2ZrCuO_4$ (Ref. 28)]. Therefore, taking into account both the frustration effects and the small exchange anisotropy near the transition point can be important for the analysis of the experimental data related to these compounds.

In the isotropic case of Eq. (1), the ground state for $0<J<1/4$ is ferromagnetic state, degenerated with respect to total $S^z$. Weak easy-plane anisotropy $\Delta_1,\Delta_2<1$ lifts this degeneracy, and the ground state is in the sector with total $S^z=0$ at small $J$. One can expect that the increase of $J$ induces the phase transition at some $J_c$ to the incommensurate phase with $S^z=0$. Besides, the character of this transition can be different from that in the isotropic case.

In our analysis, we focus on the behavior of the F-AF model (1) near the transition point from the commensurate to the incommensurate ground state and the influence of the weak anisotropic interaction on the $T=0$ phase diagram. For simplicity, we concentrate our attention on the particular case of the Hamiltonian (1) with $\Delta_2=1$,

$$H=-\sum\left(S_n^xS_{n+1}^x+S_n^yS_{n+1}^y+\Delta S_n^zS_{n+1}^z-\frac{1}{4}\right)$$
$$+J\sum\left(\mathbf{S}_n\cdot\mathbf{S}_{n+2}-\frac{1}{4}\right). \qquad (2)$$

(We added here constants for convenience.)

However, we will show that the results for model (1) with both $\Delta_1\neq1$ and $\Delta_2\neq1$ are qualitatively similar to those for model (2).

The paper is organized as follows. In Sec. II, we consider a qualitative physical picture of the ground-state phase diagram of model (2) based on the classical approximation. In Sec. III, we study the phase diagram of model (2) using the variational mean-field approach. The scaling estimates of the perturbation theory for the easy-plane case of model (2) for $J<1/4$ are presented in Sec. IV. In Sec. V, we estimate infrared divergencies in the perturbation theory near the transition point $J=1/4$. Section VI is devoted to the phase transition in the easy-axis case of model (2). In Sec. VII, we present the phase diagram of model (1) in the case $\Delta_1=\Delta_2$ and summarize our results.

 

## II. CLASSICAL APPROXIMATION

Let us start from the classical picture of the ground state of model (2). In the classical approximation, the spins are vectors which form the spiral structure with a pitch angle $\varphi$ between neighboring spins and canted angle $\theta$

$$S_n^x = \frac{1}{2}\cos(\varphi n)\sin\theta,$$

$$S_n^y = \frac{1}{2}\sin(\varphi n)\sin\theta,$$

$$S_n^z = \frac{1}{2}\cos\theta. \tag{3}$$

The classical energy per site is

$$\frac{E_{\mathrm{cl}}(\varphi,\theta)}{N} = \frac{1-\Delta}{4} + \frac{\sin^2\theta}{4}\{\Delta - \cos\varphi - J[1-\cos(2\varphi)]\}. \tag{4}$$

The minimization of energy [Eq. (4)] over the angles $\varphi$ and $\theta$ shows that there are three regions in $(J, \Delta)$ having different classical energies. In region I ($J<\frac{1}{4}$, $\Delta<1$), the energy is minimized by the choice of the angles $\varphi=0$ and $\theta=\frac{\pi}{2}$. These angles correspond to the spin configuration with all spins pointing along the $x$ axis, and the energy is

$$E_{\mathrm{cl},xy} = 0. \tag{5}$$

In region II ($J<\frac{1}{4}$, $\Delta>1$) and [$J>\frac{1}{4}$, $\Delta-1>\frac{2}{J}(J-\frac{1}{4})^2$], the minimum of the energy is given by the angle $\theta=0$ (and arbitrary $\varphi$). This is the fully polarized state with all spins up (or down), and the energy

$$E_{\mathrm{cl},z} = -N\frac{\Delta-1}{4}. \tag{6}$$

In region III [$J>\frac{1}{4}$, $\Delta-1<\frac{2}{J}(J-\frac{1}{4})^2$], the classical approximation shows helical spin structure in the $x$-$y$ plane. The corresponding angles are

$$\varphi = \cos^{-1}\frac{1}{4J},$$

$$\theta = \frac{\pi}{2}, \tag{7}$$

and the classical ground-state energy

$$E_{\mathrm{cl,sp}} = -\frac{N}{2J}\left(J-\frac{1}{4}\right)^2. \tag{8}$$

The phase boundaries in the classical approximation for model (2) are shown in Fig. 1 by thin dashed lines. One can see from Fig. 1 that the transition between phases I and II takes place on the isotropic line $\Delta=1$. This transition is a simple spin flop, which is certainly of the first-order type. In the easy-axis case $\Delta>1$, the increase of the NNN exchange $J$ leads to the first-order transition to the helical phase III on the transition line,

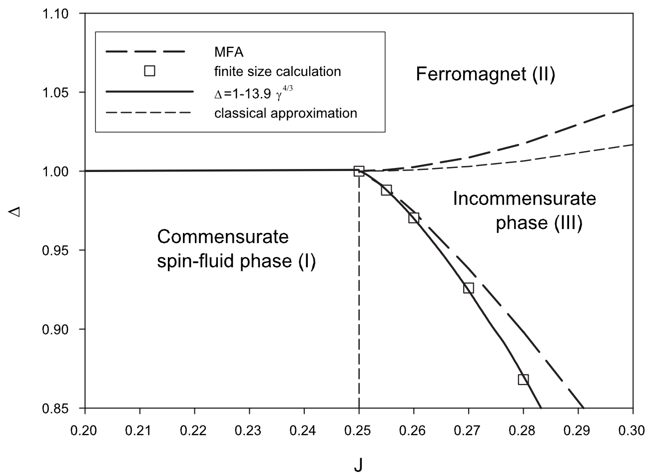


FIG. 1. The phase diagram of model (2). The phase boundaries are shown by thin dashed lines in the classical approximation and by thick dashed lines in the mean-field approach. Empty squares denote the phase transition points found by finite-size calculations and thick solid line is the transition line given by Eq. (71).

$$\Delta - 1 = \frac{2}{J}\left(J-\frac{1}{4}\right)^2. \tag{9}$$

The pitch angle $\varphi$ on this line has a finite value, which is according to Eqs. (7) and (9),

$$\varphi = [8(\Delta-1)]^{1/4}, \tag{10}$$

as $\Delta\to 1$. In contrast to the easy-axis case, in the easy-plane part of the phase diagram, the transition to the helical phase occurs at $J=1/4$, where the pitch angle $\varphi=0$, indicating the second-order type of this transition.

The phase diagram in the classical approximation is qualitatively true. However, as it will be shown below, this approximation does not give the correct behavior of the boundaries between different phases.

## III. MEAN-FIELD APPROACH

To study model (2), we use the variational mean-field approach (MFA) developed in Refs. 21 and 29. According to this approach, we follow the classical picture and transform the local axes on $n$th site by a rotation about the $z$ axis by $\varphi n$ and then by a rotation about the $y$ axis by $\theta$. The transformation to spin-1/2 operators $\eta_n$ has a form

$$\mathbf{S}_n = R_z(\varphi n)R_y(\theta)\eta_n, \tag{11}$$

where $R_y(\theta)$ and $R_z(\varphi n)$ are the operators of the corresponding rotations.

The second step is the Jordan-Wigner transformation to the obtained Hamiltonian in terms of the $\eta$ operators. This transformation maps the $\eta$-spin model onto the model of interacting spinless fermions, which is then treated by the mean-field approximation including superconductorlike correlations. The pitch and canted angles $\varphi$ and $\theta$ are variational parameters in this approach. We omit here the details of this approach because it is simple modification of what was done in Refs. 21 and 29, and we present only the results.

Generally, the phase diagram of model (2) in the MFA contains the same three phases as predicted by the classical approximation, and the boundaries between the phases are shown in Fig. 1 by thick dashed lines. In region I (see Fig. 1), the MFA shows the nonzero magnetization in the easy $x$-$y$ plane. In region II, the fully polarized state $|\uparrow\uparrow\cdots\uparrow\rangle$ represents the ground state. In region III, the MFA shows helical spin structure in the $x$-$y$ plane. However, as can be seen in Fig. 1, the boundary between the phases I and III is substantially shifted. In the MFA, this boundary in the vicinity of the point ($J=\frac{1}{4}$, $\Delta=1$) is approximately given by

$$\alpha \approx 8.05\gamma^{1.25}, \tag{12}$$

where $\alpha=1-\Delta$ and $\gamma=J-\frac{1}{4}$.

The boundary between the phases II and III in the MFA is described by the equation

$$\Delta \approx 1 + 6.3\gamma^{1.7}. \tag{13}$$

Certainly, there is no long range order (LRO) in the $x$-$y$ plane in phases I and III, and in this respect, the MFA is incorrect. However, the MFA gives a good estimate for the ground-state energy in those phases. For example, in phase I at $J=0$, the MFA reproduces correctly the nontrivial critical exponent for the ground-state energy,

$$\delta E_0 \approx -0.063N\alpha^{3/2}. \tag{14}$$

This estimate differs by 16% from the exact result,[30]

$$\delta E_0 = -\frac{N\alpha^{3/2}}{3\sqrt{2}\pi}. \tag{15}$$

The MFA shows that the critical exponent $3/2$ for the ground-state energy remains up to the point $J=1/4$, where the behavior of the ground-state energy is changed to

$$\delta E_0 \approx -0.07N\alpha^{9/7}. \tag{16}$$

As was shown in Ref. 21, the MFA gives also a good estimate for a critical exponent of the ground-state energy in the isotropic case $\Delta=1$ of the helical phase III,

$$\delta E_0 \approx -1.585N\gamma^{12/7}. \tag{17}$$

As will be shown below, the estimates of the ground-state energies and the phase boundaries in the MFA given by Eqs. (12) and (13) are in a good accordance with scaling estimates and finite-size calculations.

## IV. PERTURBATION THEORY FOR EASY-PLANE CASE AT $J<1/4$

We are interested in the behavior of model (2) in the vicinity of the isotropic case $\Delta=1$. For this aim, it is natural to develop the perturbation theory (PT) in small parameter $\alpha=1-\Delta$,

$$H = H_0 + V_J + V_\alpha,$$

$$H_0 = -\sum\left(\mathbf{S}_n\cdot\mathbf{S}_{n+1} - \frac{1}{4}\right),$$

$$V_J = J\sum\left(\mathbf{S}_n\cdot\mathbf{S}_{n+2} - \frac{1}{4}\right),$$

$$V_\alpha = \alpha\sum S_n^z S_{n+1}^z. \tag{18}$$

At first, let us consider the most simple case $J=0$, where the ground-state energy at $\alpha\ll 1$ is given by Eq. (15). The ground state of $H_0$ is ferromagnetic and is degenerate with respect to total $S^z$. The perturbation $V_\alpha$ splits this degeneracy, and in the first order in $\alpha$, we have

$$\langle\psi(S^z)|V_\alpha|\psi(S^z)\rangle = \frac{\alpha}{4}\frac{(4S^z-N)}{N-1}. \tag{19}$$

Thus, the first order shows that one should develop the PT for the lowest state $|\psi_0\rangle$ having total spin $S=\frac{N}{2}$ and $S^z=0$. The perturbation series for the ground-state energy can be written in a form

$$E_0(\alpha) = \langle\psi_0|V_\alpha + V_\alpha\frac{1}{E_0-H_0}V_\alpha + \cdots|\psi_0\rangle. \tag{20}$$

Suppose that the main contributions to the energy are given by low-lying excitations, which for an isotropic ferromagnet with the spectrum $\varepsilon_k=k^2/2$ behave as

$$E_k - E_0 \sim N^{-2}. \tag{21}$$

The higher orders of the perturbation series contain more dangerous denominators and, therefore, possibly have higher powers of the infrared divergency. Therefore, we use scaling arguments to estimate the critical exponent for the ground-state energy. Below, we will pay attention only to the powers of the divergent terms and omit numerical factors.

Let us assume that the matrix elements of the perturbation operator $V_\alpha$ between low-lying states $|\psi_n\rangle$ involved in the PT (having $S^z=0$ but different total $S$) at $N\to\infty$ behave as

$$\langle\psi_i|V_\alpha|\psi_j\rangle \sim \alpha. \tag{22}$$

Collecting the most divergent parts in all orders of the PT, we express the correction to the ground-state energy as

$$E_0(\alpha) = \langle\psi_0|V_\alpha|\psi_0\rangle\sum_{m=0}^{\infty} c_m x^m = \alpha f_\alpha(x), \tag{23}$$

where $c_m$ are unknown constants and

$$x \sim \frac{\langle\psi_i|V_\alpha|\psi_k\rangle}{E_k-E_0} \sim \alpha N^2 \tag{24}$$

is a scaling parameter, which absorbs the infrared divergencies.

The scaling function $f_\alpha(x)$ at $x\to 0$ is given by the first-order correction. In the thermodynamic limit ($x\to\infty$), the behavior of $f_\alpha(x)$ is generally unknown, but the natural condition $E_0(\alpha)\sim N$ at $N\to\infty$ requires

$$f_\alpha(x) \sim \sqrt{x} \tag{25}$$

and, finally,

$$E_0(\alpha) \sim -N\alpha^{3/2}. \quad (26)$$

The obtained expression is in agreement with the exact equation [Eq. (15)] for the ground-state energy, which justifies our assumption about the behavior of the matrix elements [Eq. (22)].

Moreover, exploiting the fact that the system in region $\Delta<1$ is in a spin-fluid phase, the correction to the ground-state energy has a form[31]

$$E_0 = Ne_0 - \frac{\pi c v_{\text{sound}}}{6N}, \quad (27)$$

where $e_0$ is the ground-state energy at $N\to\infty$ and the central charge is $c=1$ in our case. In order to reproduce such $1/N$ correction to the energy, the asymptotic of $f_\alpha(x)$ at large $x$ should have a form

$$f_\alpha(x) = a\sqrt{x} + \frac{b}{\sqrt{x}}, \quad (28)$$

with some constants $a$ and $b$. So, from Eq. (23), we find

$$E_0(\alpha) = -Na\alpha^{3/2} - \frac{b\alpha^{1/2}}{N} \quad (29)$$

and, therefore,

$$v_{\text{sound}} \sim \sqrt{\alpha}, \quad (30)$$

which agrees with an exact result $v_{\text{sound}}=\sqrt{\alpha/2}$ at $\alpha\ll 1$.[32] Thus, the scaling estimates give us the correct exponent for the sound velocity as well.

Now, let us consider PT [Eq. (18)] containing both channels $V_\alpha$ and $V_J$. Each channel can produce infrared divergencies and is described by its own scaling parameter.[34] We have already obtained the scaling parameter $x\sim\alpha N^2$ for the perturbation $V_\alpha$, and now, we are going to determine the scaling parameter for the perturbation $V_J$. For this aim, one needs to know the $N$ dependence of the matrix elements $\langle\psi_i|V_J|\psi_j\rangle$. In general, it is unknown. However, one can restore these matrix elements from the known exact expression for NNN spin correlator in the ground state $|\psi_0(\alpha)\rangle$ at $J=0$ and some small value of $\alpha$:[33]

$$\langle\psi_0(\alpha)|\left(\mathbf{S}_n\cdot\mathbf{S}_{n+2} - \frac{1}{4}\right)|\psi_0(\alpha)\rangle = -\frac{\sqrt{2}}{3\pi}\alpha^{3/2} \quad (31)$$

or, in other words,

$$\langle\psi_0(\alpha)|V_J|\psi_0(\alpha)\rangle = -\frac{\sqrt{2}}{3\pi}\alpha^{3/2}JN. \quad (32)$$

On the other hand, collecting all contributions of the PT to the linear term in $J$ similar to what was done in Eq. (23), we arrive at a scaling form in small parameter $\alpha$,

$$\langle\psi_0(\alpha)|V_J|\psi_0(\alpha)\rangle \sim \langle\psi_i|V_J|\psi_j\rangle f_J(x), \quad (33)$$

with $x=\alpha N^2$.

The comparison of Eqs. (32) and (33) immediately leads to the results

$$\langle\psi_i|V_J|\psi_j\rangle \sim JN^{-2} \quad (34)$$

and

$$f_J(x) \sim x^{3/2}. \quad (35)$$

So, the matrix elements $\langle\psi_i|V_J|\psi_j\rangle$ are small enough to eliminate dangerous denominators,

$$y \sim \frac{\langle\psi_i|V_J|\psi_j\rangle}{E_k - E_0} \sim J, \quad (36)$$

which, in turn, implies the absence of infrared divergencies in $V_J$ channel. Thus, the perturbation $V_J$ does not form a scaling parameter, and the ground-state energy has regular expansion in $J$.

It is natural to expect that the behavior of the matrix elements of type (34) remains the same up to the point $J=1/4$. It results in the following expression for the ground-state energy for $J<1/4$:

$$E_0 = -N\alpha^{3/2}g_J(J), \quad (37)$$

where $g_J(J)$ is some unknown smooth function, which at small $J$ has the expansion in accordance with the exact results [Eqs. (15) and (32)],

$$E_0 = -\frac{N\alpha^{3/2}}{3\sqrt{2}\pi}(1+2J). \quad (38)$$

However, as $J\to 1/4$, one should take into account that the excitation spectrum is $\varepsilon_k=\left(\frac{1}{2}-2J\right)k^2$ and the excitation energies become

$$E_k - E_0 \sim \frac{\frac{1}{4}-J}{N^2}. \quad (39)$$

This modifies the scaling parameter,

$$x \sim \frac{\alpha N^2}{\frac{1}{4}-J}, \quad (40)$$

and the expression for the energy,

$$E_0 \sim -\frac{N\alpha^{3/2}}{\sqrt{\frac{1}{4}-J}}. \quad (41)$$

Similarly, the sound velocity at $J\to 1/4$ behaves as

$$v_{\text{sound}} \sim \sqrt{\frac{1}{4}-J}\sqrt{\alpha}. \quad (42)$$

## V. PERTURBATION THEORY NEAR THE TRANSITION POINT $J=1/4$, $\Delta=1$

At $J=1/4$ and $\Delta=1$, the ferromagnetic ground state becomes degenerate with a singlet spiral state.[25] For $\Delta<1$, the ground state obviously lies in the $S^z=0$ sector. Therefore, in order to determine the transition line between phases I and III, one should develop the PT both to the ferromagnetic state with $S^z=0$ and to the singlet spiral state.

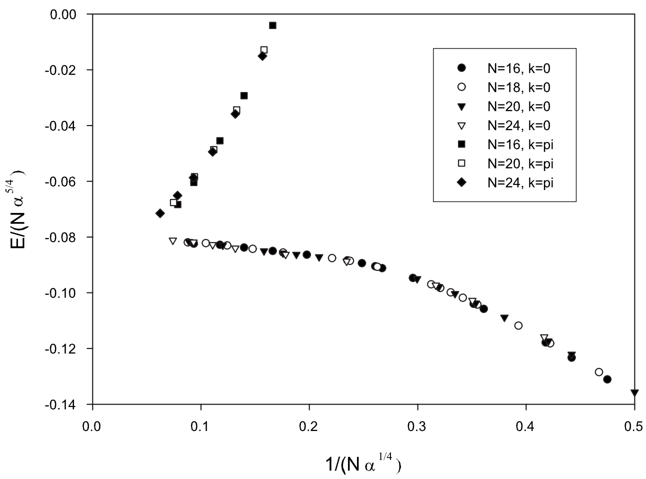


FIG. 2. The scaling function $f(x)$ in Eq. (46) for the ground-state energy and the lowest excited state at $J=1/4$.

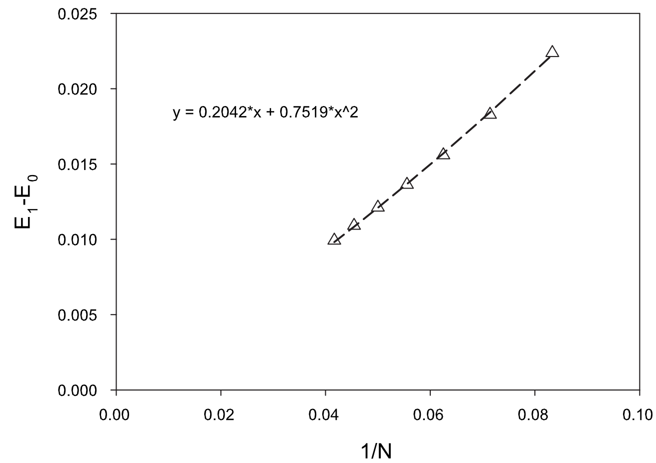


FIG. 3. $N$ dependence of the energy gap between the ground state and the lowest excitation of model (2) at $J=1/4$ and $\Delta=0.96$.

### A. Perturbation theory to the ferromagnetic state with $S^z=0$

Let us represent the Hamiltonian in a form

$$H = H_0 + V_\alpha + V_\gamma,$$

$$H_0 = -\sum\left(\mathbf{S}_n\cdot\mathbf{S}_{n+1}-\frac{1}{4}\right)+\frac{1}{4}\sum\left(\mathbf{S}_n\cdot\mathbf{S}_{n+2}-\frac{1}{4}\right),$$

$$V_\alpha = \alpha\sum S_n^z S_{n+1}^z,$$

$$V_\gamma = \gamma\sum\left(\mathbf{S}_n\cdot\mathbf{S}_{n+2}-\frac{1}{4}\right). \tag{43}$$

We assume that the behavior of the matrix elements of operators $V_\alpha$ and $V_\gamma$ remains the same as in region $J<1/4$ [see Eqs. (22) and (34)]. However, the scaling parameters are modified due to the changes in one-particle excitation spectrum, which is $\varepsilon_k=k^4/8$ at $J=1/4$.[10] So, the low-lying excited states involved in PT [Eq. (43)] behave as

$$E_k - E_0 \sim N^{-4}. \tag{44}$$

Now, according to Eqs. (24) and (36), both channels $V_\alpha$ and $V_\gamma$ produce the scaling parameters,

$$x = \alpha N^4,$$

$$y = \gamma N^2. \tag{45}$$

Thus, as follows from Eq. (23) exactly at $J=1/4$ ($y=0$), the ground-state energy can be written in a scaling form

$$E_0(\alpha) = -N\alpha^{5/4}f(x). \tag{46}$$

This scaling and the critical exponent are confirmed by numerical calculations, where the function $f(x)$ is calculated on finite chains with different $N$ and $\alpha$ for the ground state with $k=0$ (see Fig. 2). As one can see in Fig. 2, all data lie perfectly on one curve $f(x)$ and in the thermodynamic limit, the function $f(x)\to 0.08$. We show in Fig. 2 that the same scaling [Eq. (46)] is valid for the lowest excited state with $k=\pi$ as well and that the corresponding scaling function has the same thermodynamic limit $f(x)\to 0.08$.

The system at $J=1/4$ and $\alpha>0$ is in a spin-fluid phase, which is verified by $1/N$ behavior of low-lying excitations calculated on finite chains (see Fig. 3). From the scaling [Eq. (46)], we can extract also the critical exponent for the sound velocity

$$v_{\text{sound}} \sim \alpha^{3/4}. \tag{47}$$

In case when both $V_\alpha$ and $V_\gamma$ act simultaneously, the scaling estimates [Eq. (45)] give

$$E_0(\alpha,\gamma) = -N\alpha^{5/4}f(x,y). \tag{48}$$

In the thermodynamic limit, when both $x\to\infty$ and $y\to\infty$, the scaling function $f(x,y)$ becomes a function of one variable (independent of $N$),

$$\nu = \frac{y^2}{x} = \frac{\gamma^2}{\alpha}, \tag{49}$$

and the ground-state energy takes a form

$$E_0(\alpha,\gamma) = -N\alpha^{5/4}g(\nu). \tag{50}$$

### B. Perturbation theory to the singlet spiral state

The PT to the singlet spiral state with pitch angle $\varphi$ in the isotropic case $\alpha=0$ was developed in Ref. 34, where it was found that the energy has a scaling form

$$E(0,\gamma,\varphi) = -N\frac{\gamma\varphi^2}{2} + N\varphi^5 f(\gamma N^2,\varphi N), \tag{51}$$

where the first term comes from the first order of the PT in $\gamma$ and the second one originates from the scaling estimates of the infrared divergencies of higher orders of the PT. Comparison of Eqs. (48) and (51) leads to a general expression for the energy, which correctly reduces to both cases at $\varphi\to 0$ and $\alpha\to 0$,

$$E(\alpha,\gamma,\varphi) = -N\frac{\gamma\varphi^2}{2} + N\varphi^5 f(\alpha N^4,\gamma N^2,\varphi N) \qquad (52)$$

(in fact, this equation can be derived in a similar manner as was done in Ref. 34).

In the thermodynamic limit, when all variables in the scaling function in Eq. (52) tends to infinity, the scaling dependence transforms to a function of two variables,

$$E(\alpha,\gamma,\varphi) = -N\frac{\gamma\varphi^2}{2} + N\varphi^5 g(\mu,\nu), \qquad (53)$$

where

$$\mu = \frac{\alpha}{\varphi^4},$$

$$\nu = \frac{\gamma^2}{\alpha}. \qquad (54)$$

Generally, the function $g(\mu,\nu)$ is unknown. However, we can identify some of its properties. At first, in the limit $\varphi \to 0$, we should reproduce Eq. (50). Moreover, in the spin-fluid phase, the spiral states with $\varphi \sim N^{-1}$ should describe soundlike excitations with the sound velocity [Eq. (47)]. These requirements suggest that in the limit $\mu\to\infty$, the function $g(\mu,\nu)$ has an asymptotic behavior,

$$\lim_{\mu\to\infty} g(\mu,\nu) \sim -\mu^{5/4}g_1(\nu) + \mu^{3/4}g_2(\nu) + o(\mu^{3/4}). \qquad (55)$$

One can check that this expression reproduces the soundlike excitations at $\gamma=0$,

$$E(\alpha,0,\varphi) - E(\alpha,0,0) \sim N\alpha^{3/4}\varphi^2 \sim \frac{\alpha^{3/4}}{N}. \qquad (56)$$

In the limit $\mu\to 0$, according to Ref. 34, we have

$$\lim_{\mu\to 0} g(\mu,\nu) \sim A + o(1), \qquad (57)$$

where constant $A$ describes the excitation spectrum at the transition point $\alpha=0$ and $\gamma=0$. Finite-size calculations give for this constant the value $A\approx 0.0065$.

Summarizing all above, we extract explicitly the corresponding terms and obtain the following expression:

$$\frac{1}{N}E(\alpha,\gamma,\varphi) = -\frac{\gamma\varphi^2}{2} - \alpha^{5/4}g_1(\nu) + \alpha^{3/4}\varphi^2 g_2(\nu) + A\varphi^5 + \varphi^5 g_3(\mu,\nu), \qquad (58)$$

where the function $g_3(\mu,\nu)$ has limits

$$\lim_{\mu\to 0} g_3(\mu,\nu) \sim o(1),$$

$$\lim_{\mu\to\infty} g_3(\mu,\nu) \sim o(\mu^{3/4}). \qquad (59)$$

The minimization of energy [Eq. (58)] over the pitch angle $\varphi$,

$$\frac{\partial E(\alpha,\gamma,\varphi)}{\partial\varphi} = 0, \qquad (60)$$

gives the following equation for $\varphi_{\min}$:

$$\gamma = \varphi^3\left[5A + 2\mu^{3/4}g_2(\nu) + 5g_3(\mu,\nu) - 4\mu\frac{\partial g_3(\mu,\nu)}{\partial\mu}\right]. \qquad (61)$$

We see that in the isotropic limit $\alpha \ll \varphi^4$ $(\mu\to 0)$, the pitch angle is defined by the constant term on the right-hand side of Eq. (61) [using Eq. (59)],

$$\varphi_{\min} = \left(\frac{\gamma}{5A}\right)^{1/3}, \qquad (62)$$

which reproduces the result of Ref. 34.

In order to find the commensurate-incommensurate transition line, where the pitch angle $\varphi_{\min}$ vanish, it is more convenient to rewrite Eq. (61) in a form

$$\frac{\gamma}{\alpha^{3/4}} - 2g_2(\nu) = \frac{1}{\mu^{3/4}}\left[5A + 5g_3(\mu,\nu) - 4\mu\frac{\partial g_3(\mu,\nu)}{\partial\mu}\right]. \qquad (63)$$

From Eqs. (63) and (59), one can see that the right-hand side of Eq. (63) tends to zero at $\mu\to\infty$, which corresponds to the limit $\varphi\to 0$. The left-hand side of Eq. (63) is independent of $\varphi$ and vanishes on the transition line,

$$\gamma = 2g_2(0)\alpha^{3/4} \qquad (64)$$

(we note that on the transition line [Eq. (64)] $\nu=0$).

Hence, in approaching to the transition line [Eq. (64)], the pitch angle $\varphi_{\min}$ smoothly goes to zero. So, the line [Eq. (64)] determines the second-order transition line between the commensurate spin-fluid phase I with $\varphi=0$ and the incommensurate spiral phase III with $\varphi\neq 0$.

Another question that can be studied concerns the low-lying excitations in the incommensurate phase. According to Eq. (60), the behavior of the energy near $\varphi_{\min}$ is expanded as

$$E(\alpha,\gamma,\varphi) = E(\alpha,\gamma,\varphi_{\min}) + \frac{(\varphi-\varphi_{\min})^2}{2}\frac{\partial^2 E(\alpha,\gamma,\varphi)}{\partial\varphi^2}. \qquad (65)$$

The second-order derivative of the energy at $\varphi=\varphi_{\min}$ can be estimated as

$$\frac{\partial^2 E(\alpha,\gamma,\varphi_{\min})}{\partial\varphi^2} \sim N\gamma. \qquad (66)$$

Thus, the states with

$$\varphi_k = \varphi_{\min} \pm \frac{2\pi}{N}k \qquad (67)$$

describe gapless excitations with the energy

$$\delta E \sim \frac{\gamma}{N}. \qquad (68)$$

Certainly, there is no helical LRO in the spiral phase, and the spin correlations decay on large distances. However, the nature of the spiral phase manifests itself in the incommensurate position $q_{\max}$ of the maximum of structure factor,

$$S(q) = \sum_{n,r} e^{iqr} \langle \mathbf{S}_n \cdot \mathbf{S}_{n+r} \rangle . \tag{69}$$

When the $O(3)$ rotation symmetry is broken by the anisotropic term $V_\alpha$, the incommensurate nature of the spiral phase remains in the $x$-$y$ plane. So, in this case, we associate the pitch angle of the spiral $\varphi$ with the position of maximum of the structure factor $q_{\max}$ in the easy plane,

$$S^{xx}(q) = \sum_{n,r} e^{iqr} \langle S_n^x S_{n+r}^x + S_n^y S_{n+r}^y \rangle . \tag{70}$$

The numerical calculations on finite chains show that for a fixed small value of $\gamma$, the finite-$N$ value of $q_{\max}(N)$ decreases stepwise by the amount $\frac{2\pi}{N}$ from some finite value at $\alpha=0$ to zero on the transition line, when $\alpha$ is

$$\alpha \approx 13.9\gamma^{4/3} . \tag{71}$$

On this line, the incommensurate phase III terminates (see Fig. 1) and the transition into commensurate spin-fluid phase takes place. Thus, the numerical calculation confirms the found critical exponent for the transition line [Eq. (64)]. The fact that the pitch angle $\varphi$ tends to zero at approaching to the transition line ensures that this line is the second-order transition.

## VI. EASY-AXIS CASE

In the easy-axis case for $J<1/4$, the fully polarized state $|\uparrow\uparrow\cdots\uparrow\rangle$ is evidently the ground state. In region $J>1/4$, one should compare the fully polarized state energy with the energy of the spiral state. The finite-size numerical calculations show that for a fixed small $\gamma$, the increasing of easy-axis anisotropy leads to the decrease of the pitch angle $\varphi$, but the ground state remains in the sector with total $S^z=0$. At some critical value of $\Delta_c$, the transition from the state with $S^z=0$ and some finite value of the pitch angle $\varphi$ to the fully polarized state occurs. Thus, in contrast to the easy-plane case, the transition from the spiral phase to the ferromagnetic phase is the first-order one.

The finite-size numerical calculations also show that in the spiral region $1<\Delta<\Delta_c$, it is sufficient to take into account only the first-order correction in $(\Delta-1)$ to the spiral state. That is, the energy of the spiral state is

$$E_{sp} = -aN\gamma^{5/3} - N\frac{\Delta-1}{12}, \tag{72}$$

and the transition to the fully polarized state with the energy,

$$E_f = -N\frac{\Delta-1}{4}, \tag{73}$$

takes place at

$$\Delta_c = 1 + 6a\gamma^{5/3} . \tag{74}$$

Unfortunately, the factor $a$ in Eq. (74) cannot be determined by finite-size calculations because of the irregular behavior of $\Delta_c$ with $N$. However, we believe that the MFA gives a good estimate for this transition line [Eq. (13)].

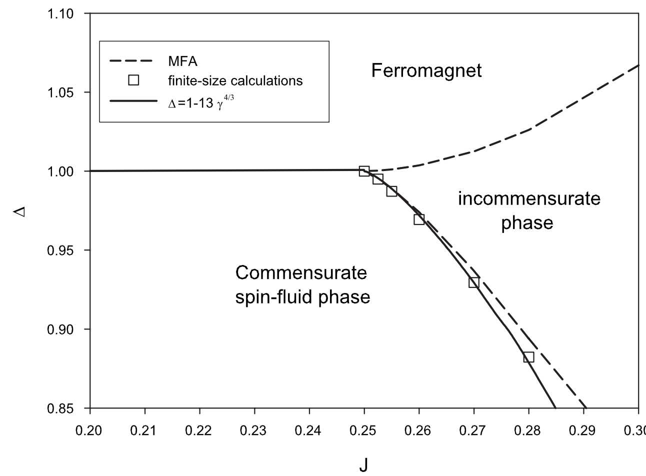


FIG. 4. The phase diagram of model (1) with $\Delta_1=\Delta_2=\Delta$. The phase boundaries are shown by dashed lines in the mean-field approach. Empty squares denote the phase transition points found by finite-size calculations and thick solid line is the fitting line to these points.

## VII. SUMMARY

We have studied spin-1/2 zigzag chain with weakly anisotropic ferromagnetic nearest-neighbor and antiferromagnetic next-nearest-neighbor interactions. It was shown that the ground-state phase diagram consists of three phases: the fully polarized ferromagnetic phase, the commensurate spin-fluid phase, and the incommensurate phase. Thus, the incommensurate phase established for the isotropic case survives weak anisotropy of interactions, though in this case, the incommensurate nature of the ground state reveals itself in the $x$-$y$ plane.

Using scaling estimates of the infrared divergencies in the perturbation theory, we obtained the scaling expression for the ground-state energy both for commensurate and incommensurate phases. This allowed us to determine nontrivial critical exponents in the behavior of the phase transition lines, which were confirmed by finite-size calculations. We found also that in the easy-plane case, the transition from the commensurate spin-fluid to the incommensurate phase is of the second-order one, while in the easy-axis case, the transition from the fully polarized state with $S^z=S^z_{max}$ to the incommensurate state with $S^z=0$ is evidently of the first order.

In this paper, we have focused on model (2), which is a particular case of the more general model (1). However, the obtained results for model (2) remain valid at least qualitatively for model (1). The reason is that the matrix elements of the operators $\Sigma S_n^z S_{n+1}^z$ and $\Sigma S_n^z S_{n+2}^z$ have the same $N$ behavior. Therefore, in general case, a variable $(\Delta_2-1)/(\Delta_1-1)$ will appear in the scaling functions [Eqs. (50) and (53)], but all obtained scaling properties and the critical exponents of the system remain the same. As an example, we present in Fig. 4 the phase diagram near the transition point $J=1/4$ of model (1) for the particular case $\Delta_1=\Delta_2$. We see that the phase diagram in this case is very similar even quantitatively to that shown in Fig. 1.

There is one remark related to the phase diagram in Fig. 4. Our analysis shows that for $J$ close to the transition point

$J=1/4$, the incommensurate phase exists for both cases $\Delta<1$ and $\Delta>1$ and the pitch angle is a smooth function of $\Delta$ in the vicinity of $\Delta=1$. We note that similar smooth behavior of the pitch angle near the isotropic case has been observed for the model with both AF NN ($J_1>0$) and NNN ($J_2>0$) interactions and $\Delta_1=\Delta_2=\Delta$.[36] At the same time, as was suggested in Ref. 26, the phases in the easy-axis and the easy-plane cases can be different: for $\Delta>1$, the system has AF LRO of the type $\uparrow\uparrow\downarrow\downarrow$ in contrast to the case $\Delta<1$, when there is no AF LRO. On the other hand, the classical approximation shows that the transition from the incommensurate phase to the AF phase takes place at $\Delta=1+\frac{1}{8J^2}$, which lies out of the range shown in Fig. 4. Certainly, quantum fluctuations can substantially change the classical phase diagram.

As we noticed, the used approach is valid for values of $J$ not too far from the transition point $J=1/4$, and it is unclear what happens with the incommensurate and AF phases in the region of large values of $J$. Therefore, an important and interesting question about the boundaries of the incommensurate phase and the possibility of the commensurate-incommensurate transition in the region of large values of $J$ is out of scope of this paper and requires further studies.

## ACKNOWLEDGMENTS

We would like to thank S.-L. Drechsler and D. Baeriswyl for valuable comments related to this work. D.V.D. thanks the University of Fribourg for kind hospitality. D.V.D. was supported by INTAS YS under Grant No. 05-109-4916. The numerical calculations were carried out with use of the ALPS libraries (Ref. 35). This work was supported under RFBR Grant No. 08-02-00278.

*dmitriev@deom.chph.ras.ru


[1] H.-J. Mikeska and A. K. Kolezhuk, in *Quantum Magnetism*, edited by U. Schollwöck, J. Richter, D. J. J. Farnell, and R. F. Bishop, Lecture Notes in Physics Vol. 645 (Springer-Verlag, Berlin, 2004), p. 1.

[2] F. D. M. Haldane, Phys. Rev. B **25**, R4925 (1982).

[3] T. Tonegawa and I. Harada, J. Phys. Soc. Jpn. **56**, 2153 (1987).

[4] K. Nomura and K. Okamoto, Phys. Lett. A **169**, 433 (1992).

[5] R. Bursill, G. A. Gehring, D. J. J. Farnell, J. B. Parkinson, T. Xiang, and C. Zeng, J. Phys.: Condens. Matter **7**, 8605 (1995).

[6] C. K. Majumdar and D. K. Ghosh, J. Math. Phys. **10**, 1388 (1969).

[7] S. R. White and I. Affleck, Phys. Rev. B **54**, 9862 (1996).

[8] T. Tonegawa and I. Harada, J. Phys. Soc. Jpn. **58**, 2902 (1989).

[9] A. V. Chubukov, Phys. Rev. B **44**, R4693 (1991).

[10] V. Ya. Krivnov and A. A. Ovchinnikov, Phys. Rev. B **53**, 6435 (1996).

[11] F. Heidrich-Meisner, A. Honecker, and T. Vekua, Phys. Rev. B **74**, 020403(R) (2006).

[12] H. T. Lu, Y. J. Wang, S. Qin, and T. Xiang, Phys. Rev. B **74**, 134425 (2006).

[13] A. A. Nersesyan, A. O. Gogolin, and F. H. L. Essler, Phys. Rev. Lett. **81**, 910 (1998).

[14] R. Jafari and A. Langari, Phys. Rev. B **76**, 014412 (2007).

[15] Y. Mizuno, T. Tohyama, S. Maekawa, T. Osafune, N. Motoyama, H. Eisaki, and S. Uchida, Phys. Rev. B **57**, 5326 (1998).

[16] M. Enderle, C. Mukherjee, B. Fak, R. K. Kremer, J.-M. Broto, H. Rosner, S.-L. Drechsler, J. Richter, J. Malek, A. Prokofiev, W. Assmus, S. Pujol, J.-L. Raggazzoni, H. Rakoto, M. Rheinstaedter, and H. M. Ronnow, Europhys. Lett. **70**, 237 (2005).

[17] S.-L. Drechsler, J. Richter, A. A. Gippius, A. Vasiliev, A. A. Bush, A. S. Moskvin, J. Malek, Y. Prots, W. Schnelle, and H. Rosner, Europhys. Lett. **73**, 83 (2006).

[18] M. Hase, H. Kuroe, K. Ozawa, O. Suzuki, H. Kitazawa, G. Kido, and T. Sekine, Phys. Rev. B **70**, 104426 (2004).

[19] S.-L. Drechsler, J. Richter, R. Kuzian, J. Malek, N. Tristan, B. Buechner, A. S. Moskvin, A. A. Gippius, A. Vasiliev, O. Volkova, A. Prokofiev, H. Rakoto, J.-M. Broto, W. Schnelle, M. Schmitt, A. Ormeci, C. Loison, and H. Rosner, J. Magn. Magn. Mater. **316**, 306 (2007).

[20] S.-L. Drechsler, N. Tristan, R. Klingeler, B. Büchner, J. Richter, J. Malek, O. Volkova, A. Vasiliev, M. Schmitt, A. Ormeci, C. Loison, W. Schnelle, and H. Rosner, J. Phys.: Condens. Matter **19**, 145230 (2007).

[21] D. V. Dmitriev and V. Ya. Krivnov, Phys. Rev. B **73**, 024402 (2006).

[22] D. C. Cabra, A. Honecker, and P. Pujol, Eur. Phys. J. B **13**, 55 (2000).

[23] C. Itoi and S. Qin, Phys. Rev. B **63**, 224423 (2001).

[24] H. P. Bader and R. Schilling, Phys. Rev. B **19**, 3556 (1979).

[25] T. Hamada, J. Kane, S. Nakagawa, and Y. Natsume, J. Phys. Soc. Jpn. **57**, 1891 (1988); **58**, 3869 (1989).

[26] R. D. Somma and A. A. Aligia, Phys. Rev. B **64**, 024410 (2001).

[27] H.-A. Krug von Nidda, L. E. Svistov, M. V. Eremin, R. M. Eremina, A. Loidl, V. Kataev, A. Validov, A. Prokofiev, and W. Assmus, Phys. Rev. B **65**, 134445 (2002).

[28] S.-L. Drechsler, O. Volkova, A. N. Vasiliev, N. Tristan, J. Richter, M. Schmitt, H. Rosner, J. Malek, R. Klingeler, A. A. Zvyagin, and B. Buchner, Phys. Rev. Lett. **98**, 077202 (2007).

[29] D. V. Dmitriev and V. Ya. Krivnov, Phys. Rev. B **70**, 144414 (2004).

[30] C. N. Yang and C. P. Yang, Phys. Rev. **150**, 327 (1966).

[31] H. W. J. Blote, J. L. Cardy, and M. P. Nightingale, Phys. Rev. Lett. **56**, 742 (1986); I. Affleck, *ibid.* **56**, 746 (1986).

[32] J. D. Johnson, S. Krinsky, and B. M. McCoy, Phys. Rev. A **8**, 2526 (1973).

[33] G. Kato, M. Shiroishi, M. Takahashi, and K. Sakai, J. Phys. A **36**, L337 (2003).

[34] D. V. Dmitriev, V. Ya. Krivnov, and J. Richter, Phys. Rev. B **75**, 014424 (2007).

[35] F. Alet, P. Dayal, A. Grzesik, A. Honecker, M. Korner, A. Lauchli, S. R. Manmana, I. P. McCulloch, F. Michel, R. M. Noack, G. Schmid, U. Schollwock, F. Stockli, S. Todo, S. Trebst, M. Troyer, P. Werner, and S. Wessel, J. Phys. Soc. Jpn. **74**, 30 (2005).

[36] A. A. Aligia, C. D. Batista, and F. H. L. Essler, Phys. Rev. B **62**, 3259 (2000).